

Assessment of a Scalar Concentration (Komori) Probe for Measuring Fluctuating Dye Concentration in Water

J.T. Madhani, D. Pendrey, R. Situ and R.J. Brown

School of Engineering Systems
Queensland University of Technology, Brisbane, Queensland, 4000 AUSTRALIA

Abstract

The scalar (dye) concentration probe of Komori has been used at QUT to measure the dispersion of pollutants in rivers from outboard motors and the residence time distributions of stormwater quality improvement devices (SQIDs). Although usages have been documented in literature, little is known of the Komori (dye) probe's frequency response characteristics and the quality of data sampled. In this work, the frequency response characteristic of the Komori probe was determined by injecting methylene blue dye upstream of the probe flume under varying flow conditions. Despite noise and drift, the data collected from the probe provided is useful because of its high frequency response in comparison to other types of tracer measurement. The rise and fall times were reported and the theoretical response time was also determined. It was found that the frequency response is a strong function of flow velocity and a maximum of 100 Hz under typical operating conditions is determined. Comparison between rise and fall data showed that fall curve takes longer time to dissipate.

Introduction

Tracer studies are well documented and have useful applications such as measuring residence time distributions (RTD) in processing equipment, stormwater quality improvement devices (SQIDs), mixing and dispersion of pollutants etc. The majority of the experiments reported in literature use Rhodamine WT as an input tracer dye and a fluorometer to monitor the outlet concentrations in water related applications where the sensing frequency response is not critical. To study turbulent mixing between two species and to perform measurements of dye concentration fluctuations in reacting flows, Komori [3] found it necessary to use custom built scalar (dye) concentration probes (manufactured by Masatoyo P/L, Japan) with higher frequency characteristics than normally required for water related application as in environmental water flows. The custom built probe was also designed to exhibit a linear voltage response to the variation of the tracer's concentration such as coloured dye when immersed in a fluid medium. Herein, the custom built concentration probe is denoted as the Komori probe. Loberto [4] used the Komori probe to study the effect of dye mixing and dispersion in a jet stream generated by a boat propeller. As part of the ongoing research into the design improvement of SQID, the Komori probes have been employed to measure the RTD of a blocked SQID (gross pollutant trap). The Komori probes are also used to study turbulent mixing in rivers by the QUT fluid group (work unpublished). Apart from low manufacturing costs the Komori probes are easily deployable in laboratory and field studies and the tracer dye is an organic substance (methylene blue dye).

Problems have been reported in the usage of the Komori probes Loberto [4]. The probes are subjected to drift and noise particularly when sampling in unclean water. Furthermore, little is documented in relation to the Komori probe's frequency

response characteristics and the quality of data sampled. In this work, data was collected from the Komori probe by injecting dye over a range of typical flow velocities and subjected to time series analysis. Noise and frequency response were analysed. Despite noise and drift, the data collected from the probe provided is useful because of its high frequency response in comparison to other types of tracer measurement. The rise and fall times are reported and the theoretical response time was also determined. It was found that the frequency response is a strong function of the fluid flow velocity and frequency response for the rise is higher (100 Hz) than for the fall period (60Hz) under typical operating conditions.

2. Experimental Method

The experiments were performed in the 19m flume at the QUT hydraulic laboratory (figure 1). Water was supplied to the flume by a choice of three variable speed pumps at the required flow rate. The downstream weir arrangement (not illustrated) was used to regulate the water depth. A Sontek 16 MHz Micro Acoustic Doppler Velocimeter (ADV) was used to measure the mean fluid velocities. The dye measuring system comprises, a voltage supply with zero adjustment (figure 2 (a)), a Komori probe (figure 2 (b)), an injection unit and a data acquisition system (Data Translation - DT9802, not illustrated). The injection unit consists of a volumetric infusion pump (Alaris Medical Systems - formerly IVAC Corp. Model 597), a dye outlet probe and an infusion bag. The Komori probe is fabricated from a hollow stainless rod of 500 mm in length. The external diameter of the rod casing is 6 mm and attached to the probe end is a sampling volume of 75 mm³, coupled with a polarising lens (mirror), a light emitting diode and photodiode (figure 2 (c)). The end features of the Komori probe measures the opacity of the fluid in which dye is dissolved through the attenuation and reflection of light. The opacity of the fluid is a measure of dye concentration. The organic methylene blue dye is considered to be the most effective tracer substance when used with the Komori measuring system due to a linear voltage response feature. For the purpose of conducting experiments, the concentration of methylene blue dye was diluted to 25,000 p.p.m which is sufficient to allow a maximum detection of 8 p.p.m when injected and mixed into a volume of water inside the flume. The 8 p.p.m is the maximum detection range of the Komori probe. Prior to commencing measurements, the Komori probe is calibrated by measuring the output sensing voltage in clean water (0 p.p.m) and consequently in a solution of known concentration i.e. 8 p.p.m. The corrections for both the solutions (clean water and known concentration) are performed using meters and zero adjustments (labelled as "c.min" and "c.max" as shown in figure 2 (a)) on the controller (voltage supply unit). The calibration process is repeated several times.

Two sets of experiments were performed herein denoted Expt-A (higher flow rates with the infusion pump output set to 20 mL/h) and Expt-B (lower flow rates with the infusion pump output set

to 10 mL/h). Data was sampled at 20 kHz with the data acquisition system as previously described. The injection probe (figure 1) was placed upstream of the Komori concentration probe, at a distance of 50 mm for Expt-A (high flow rates) and 100 mm for Expt-B (low flow rates).

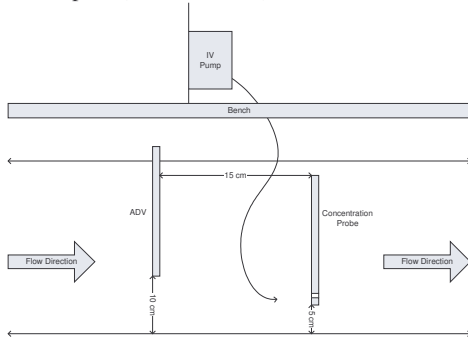


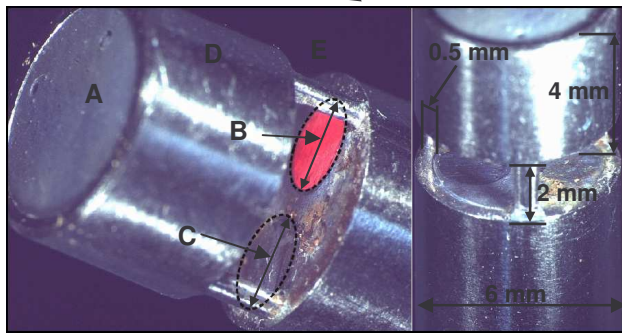
Figure 1. Frequency Response Experimental Setup



(a)



(b)



(c)

Key features: A-Polarising lens/ internal mirror, B-Light emitting diode (2 mm diameter), C-Light sensor (photodiode), (2 mm diameter), D-Sampling volume enclosure (4 mm) and E-aperture opening (2 mm).

Figure 2. The Komori (scalar dye concentration) controller (voltage supply unit) (a), the dye probe (b), the essential measurement features and the dimensions (c).

3. Frequency Response Method and Analysis

Studies relating to the frequency response characteristics of devices are well documented. For example Maffiolo [5] performed a simple response time test on chemiluminescents (CLAs) and found a typical frequency response of 1 Hz. Brown [2] applied both time domain and frequency domain methods to measure the frequency responses of the CLA which was originally developed by Mudford [6]. In the frequency domain analysis, the CLA is assumed to be a constant parameter linear system (Bendat [1], Rabiner [8]) where a linear relationship between concentration and voltage in steady state response exists. The signals from CLA and a reference cold wire (CW) were

processed using a FFT algorithm and the corresponding energy spectra obtained. While in time domain analysis, experiments were performed by specifying a step input to the CLA and finding the time constant for the response of the CLA to rise to 63.1% ($= (1 - e^{-1}) \times 100\%$) of its final value. Such methods require a known input signal which is not possible in this case. Ogata [7] lists the various attributes of outputs, and provides accurate definitions for these attributes to be measured with unusual shaped output curves.

Robinson [9] describes the frequency response measurement of a photodiode using an optical and mechanical frequency response calibrator (1 KHz to 25 Mhz). A similar approach on the Komori probe cannot be used as the effects of fluid interaction and dynamics with the probe are not considered. Furthermore the frequencies for the given range of fluid velocities are much lower than those studied by Robinson [9]. It was considered appropriate to analyse the measurement response of the Komori probe as a function of fluid velocity and to simultaneously test the reliability of the real time data series sampled. With regard to the input signal, it is assumed that the injection of dye at any instant approximates a square wave. The measuring attributes (the peak detection of dye concentration) of the Komori probe is the outcome in response (rise and fall curves) to the square wave input. For example a well defined rise and fall curve (figure 5) has a sharp peak. However, if the detection of dye is partial (figure 6) and the true measured peak is not captured the experimental data is rejected. The turbulent nature of the surrounding fluid interaction with the intrusive nature of the probe causes the dye to be only partially detected as shown in figure 6. The orientation of the probe's measuring system (light emitter diode and photodiode, see B & C in figure 2(c)) and its alignment with the direction of flow can also contribute to the partial detection of dye and in this case a distinct plateau in the rise portion of the curve is noted during experiments.

The rise and fall response times are extrapolated from the experimental data using five different methods (figure 3). The methods, described in terms of the percentage of the measured peak height (p.p.m), are classified as (0 ~ 95%), (0 ~ 1-1/e), (0 ~ 50%), (10 ~ 95%) and (5 ~ 95%) denoted herein as FrmA, FrmB, FrmC, FrmD and FrmE respectively (figure 3). Methods FrmB and C are conservative in their approach but useful if there are measurement uncertainties in detecting peak values.

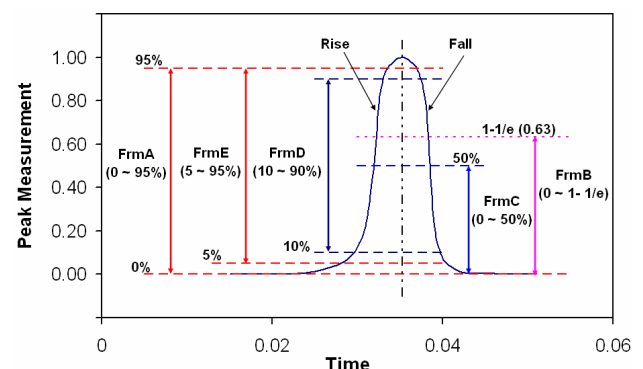


Figure 3: The frequency response methods shown in graphical form, used on data sampled by the Komori probe.

For a given flow rate the theoretical frequency response is the effective time it takes the dye to travel across the light sensor (photodiode, see C in figure 2(c)) in the sampling volume (the aperture and the sampling volume enclosure, see D & E in figure 2(c)), ignoring the interaction between the probe and the fluid. The cross sectional width of the photodiode is 2 mm and the height of the sampling volume (SV) is 6 mm. The effective time

i.e. the theoretical frequency response time (FrmT (secs)) is expressed as follows:

$$FrmT = \frac{D_{eff}}{v} \quad (1)$$

Where v is the fluid velocity m/s and D_{eff} (m) is the effective distance. Experimental results suggest under varying flow rates D_{eff} is a function of fluid velocity. To this extent four distinct values for D_{eff} (0.5, 1.0, 2.0 and 6.0 mm) are used in (1) to calculate FrmTs and are plotted in figure 4.

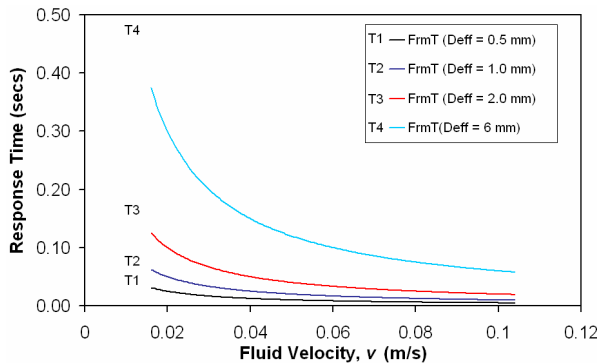


Figure 4. Theoretical frequency response curves for effective measurement width $D_{eff} = 0.5, 1, 2 \text{ \& } 6$ mm.

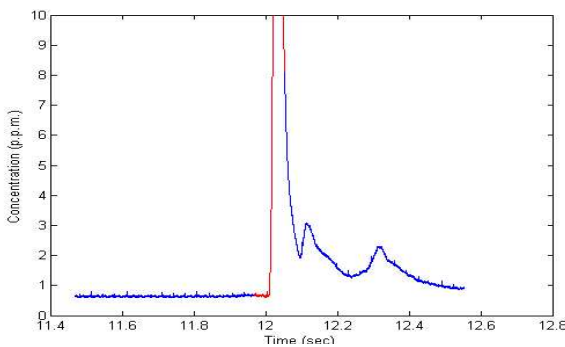


Figure 5. An typical data plot showing a sharply defined rise peak

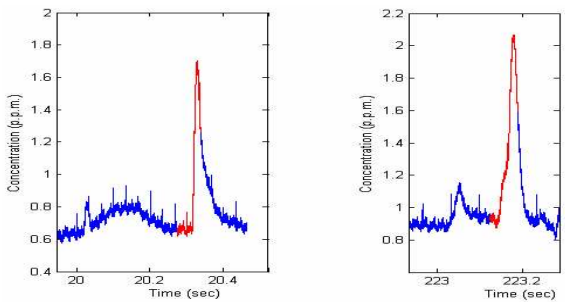


Figure 6. Typical experimental data plots showing false peaks due to the partial detection of dye.

4. Results and Discussions

Table 1 contains a summary of the number of rise and fall curves detected and the experimental setup conditions (water depth, fluid flow velocities and the flow rate of the dye pump).

The statistical mean response times for each batch of rise and fall curves are plotted in figures 7 and 8 with the theoretical response times for D_{eff} (0.5, 1, 2 and 6 mm). For purpose of graphical clarity the rise and fall plots do not have the same frequency response axes scale.

Figures 7 and 8 show that the Komori probe's frequency response characteristic to be a function of the fluid velocity. In regions where the flow velocities are greater than 0.04 m/s the data appears to be almost linear and measurement is more suitable within this range. In figure 7, the mean rise response

curves for the methods (FrmB-C) show a maximum frequency response of 100 Hz, the lowest is 60 Hz (FrmA). Similarly for the fall curves (FrmB-C) the maximum frequency response is 60 Hz and the lowest is 10 Hz (FrmA) as indicated in figure 8. It is noted from figure 7 the experimental rise data falls between $D_{eff} = 0.5$ and 1 mm. The D_{eff} for the fall curves lies between 0.5 and 6 mm (figure 8). It is unclear whether the slower response time is attributed to the retarded behaviour of the dye injected fluid dissipating from the sampling volume enclosure (see D in figure 2 (c)). Measurement uncertainties are also noted in areas relating to the probe's orientation with respect to direction of fluid flow and the surrounding flow disturbance effects. Signal noise levels in the sampling data needed to be addressed. Remedial measures were taken by using differential input connections, grounding the probe casing and using a filtering system to remove unwanted fine particles. It is unknown to what extent the residual coating of the dye on the surface of the probe casing and sensors' mounts will influence the readings. No cleaning specifications have been supplied by the manufacture to suggest otherwise.

Test	Water Depth (mm)	Water Velocity (m/s)	Dye pump flow rate (mL/h)	Rise curves (No.)	Fall curves (No.)
1	221	0.046	20	118	70
2	191	0.055	20	143	86
3	161	0.070	20	134	69
4	131	0.082	20	184	109
5	112	0.104	20	237	139
6	190	0.016	10	46	33
7	223	0.019	10	73	56
8	160	0.023	10	127	70
9	130	0.030	10	176	111

Table 1. Summary of Frequency Response Tests Performed, Expt-A (tests 1-5) and Expt-B (tests 6-9).

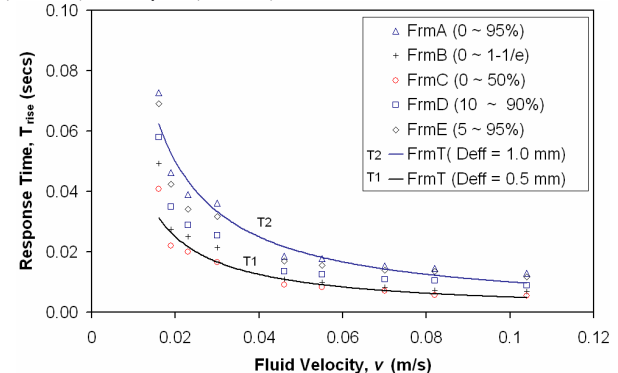


Figure 7. Comparing experimental data using the five methods (FrmA, FrmB, FrmC, FrmD, FrmE) with theoretical (FrmTs, $D_{eff} = 0.5 \text{ \& } 1.0$ mm) frequency response for the rise.

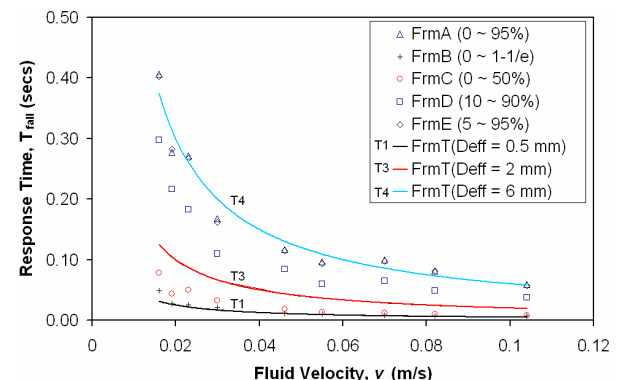


Figure 8. Comparing experimental data using the five methods (FrmA, FrmB, FrmC, FrmD, FrmE) with theoretical (FrmTs, $D_{eff} = 0.5, 2 \text{ \& } 6$ mm) frequency response for the fall.

FrmX	Rise		Fall	
	A _c (mm)	E (%)	A _c (mm)	E (%)
FrmA (0 ~ 95%)	1.05	13.0	5.94	11.0
FrmB (0 ~ 1- 1/e)	0.61	11.0	1.33	13.0
FrmC (0 ~ 50%)	0.49	11.0	0.92	14.0
FrmD (10 ~ 90%)	0.76	12.0	4.00	9.0
FrmE (5 ~ 95%)	0.95	14.0	5.85	11.0

Table 2. Rise and fall time constants using the five methods, see equation 2 & E is the measurement uncertainty (equation 3).

A power law relationship expresses the relationship between velocity and frequency response as follows:

$$FrmX(v) = A_c / v, \quad (2)$$

where $X = A, B, C, D$ or E , A_c is a constant. The measurement uncertainty (error) is expressed as:

$$E = \frac{FrmX_{predicted} - FrmX_{measured}}{FrmX_{measured}} \times 100\% \quad (3)$$

Constant A_c and the error (%) are within 95% confidence limits. The maximum and minimum rise and fall trend curves (FrmA-B) are plotted with the theoretical values (FrmT $D_{eff} = 0.5, 1, 2$ and 6 mm) in figure 9 and shows good correlation.

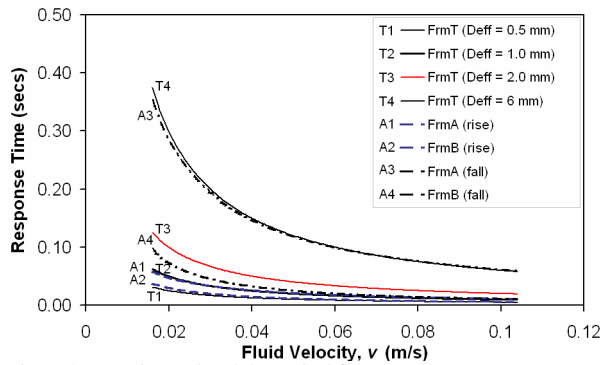


Figure 9. Experimental and theoretical frequency response curves (FrmA-B & FrmT $D_{eff} = 0.5, 1, 2$ & 6 mm) with 95% confidence prediction limits.

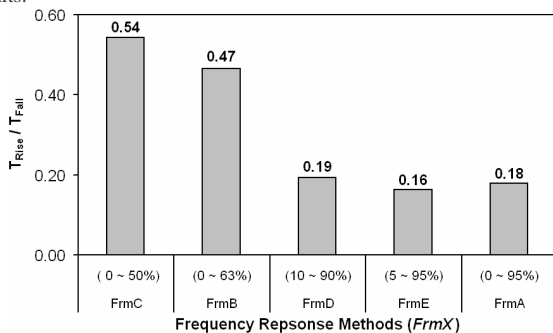


Figure 10: A histogram of the rise and fall response time ratio and the corresponding frequency response methods.

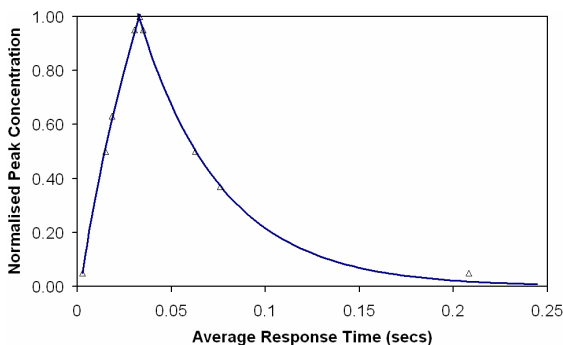


Figure 11: Average experimental rise and fall response times.

The ratio between the rise and fall data and the FrmXs are plotted in figure 10. Figure 10 initially indicates that for FrmC, the rise time is 54% of the fall time. As the response criteria changes to FrmB, there is a 7% decrease in the ratio between rise and fall data response times. When the bandwidth of response time method increases towards 90% of the measured peak value, there is a rapid increase in the fall data response time. Thereafter a stable plateau is reached where the rise time becomes less than 20% of the fall time for the remaining FrmXs i.e. FrmA, FrmD and FrmE. The fall curve has an exponential decaying behaviour towards the tail end. This is also shown in Figure 11, where the normalised peak concentration is plotted against average response time. The rise time increases rapidly while fall time decreases more slowly. Figure 11 also compares favourably with the typical signal curve as shown in Figure 5.

5. Conclusions

In this work, the frequency response characteristic of the scalar (dye) concentration probe of Komori was evaluated by injecting methylene blue dye into the flume over a range of typical flow velocities. The data sampled by the Komori probe was subjected to time series analysis and the statistical mean response times for the rise and fall curves were determined. It was found that the frequency response is a strong function of the fluid flow velocity and the maximum frequency response for the rise is higher (100 Hz) than for the fall period (60Hz) for the measured flow velocities (figures 7-8). The corresponding minimum values are 60 Hz (rise) and 10 Hz (fall). The theoretical frequency response FrmT is based on the measurement span, defined as the effective dimension D_{eff} . It was found the experimental data fitted within an effective length of $D_{eff} = 0.5$ and 6 mm. The slower fall response time may be attributed to the tendency of the injected dye to remain in the sampling volume enclosure after the peak has passed. The injected dye may also be caught in the boundary layer that forms around the probe mirror and associated surfaces. Further investigation is required to determine the influence of the sampling volume.

References

- [1] Bendat, J.S., Piersol, A.G., Random Data: Analysis and Measurement Procedures, Wiley Interscience, 1971.
- [2] Brown, R., Experimental investigation of a turbulent reacting plume, *Ph.D. Thesis* (1996), University of Sydney, Australia.
- [3] Komori, S., Hunt, J.C.R., Kanzaki, T. & Murakami, Y., The effects of turbulent mixing on the correlation between two species and on concentration fluctuations in non-premixed reacting flows, *J. Fluid Mech.* 228, 1991, 629-659.
- [4] Loberto, A.R., Brown, R.J., Kwek, M.K., Iida, A., Chanson, H. & Komori, S., An Experimental Study of the Jet of a Propellor, *Proc. 15th Australian Fluid Mechanics Conference*, University of Sydney, Sydney, 2004.
- [5] Maffiolo, G., Joos, E., Quesnel, R., & Thomas, P.F., Development and testing of short response time SO₂, NO_x and O₃ analysers, *Journal of Air Pollution and Control Association (JAPCA)* 38, 1988, 36-38.
- [6] Mudford, N.R. & Bilger, R.W., A facility for the study of nonequilibrium chemistry in an isothermal turbulent flow, *Proc. 8th Australian Fluid Mechanics Conference*, University of Newcastle, Newcastle, 1983, C.9-&C.12.
- [7] Ogata, K., Modern Control Systems (4th Edition), Prentice-Hall, 2001.
- [8] Rabiner, L.R., Gold, G., Theory and Application of Digital Signal Processing, Prentice-Hall, 1975.
- [9] Robinson, S.P., Bacon, D.R., Moss, B.C., The measurement of the frequency response of a photodiode and amplifier using an opto-mechanical frequency response calibrator, *Measurement Science and Technology*, 11, 1990, 1184.